Anisotropic thermally activated diffusion in percolation systems

S. Bustingorry[1] and G. L. Insua[2]

[1]*Consejo Nacional de Investigaciones Científicas y Técnicas, Centro Atómico Bariloche, (8400) S. C. de Bariloche, Argentina.*

[2]*Departamento de Física, Universidad Nacional del Comahue, (8300) Neuquén, Argentina.*

(Dated: February 2, 2008)

We present a study of static and frequency-dependent diffusion with anisotropic thermally activated transition rates in a two-dimensional bond percolation system. The approach accounts for temperature effects on diffusion coefficients in disordered anisotropic systems. Static diffusion shows an Arrhenius behavior for low temperatures with an activation energy given by the highest energy barrier of the system. From the frequency-dependent diffusion coefficients we calculate a characteristic frequency $\omega_c \sim 1/t_c$, related to the time t_c needed to overcome a characteristic barrier. We find that ω_c follows an Arrhenius behavior with different activation energies in each direction.

PACS numbers: 05.40.-a 05.60.Cd 66.30.-h

The study of diffusion on disordered media is an important problem, in view of its relevance in a wide variety of natural and industrial processes [1, 2, 3]. In the last years the anisotropic generalization of diffusion has attracted much attention [4, 5, 6, 7, 8, 9], justified by the diversity of systems in which diffusion takes place. A few examples of anisotropic systems are porous reservoir rocks [3, 8, 10], epoxy-graphite disk composites [11] and layered semiconducting compounds [12].

Static (long-time) and frequency-dependent conductivity on isotropic disordered media has been extensively studied with both analytical and numerical methods. One of the most widely used models for disorder media is the percolation model [3, 13, 14], due to its simplicity and interesting properties (characteristic percolation threshold, fractality of the sample-spanning cluster, etc). More recently, diffusion has also been studied in anisotropic bond percolation systems [4, 5, 7]. However, the interplay between temperature and disorder in these systems has not been studied yet. The natural manner to include temperature effects in diffusion problems is through thermally activated processes, *i.e.*, associating energy barriers to the transition rates. Interesting results are found at low temperatures in isotropic systems, where the competing effects of temperature, energy barriers and topology become important [15, 16, 17]. Static diffusion is then described by an Arrhenius law with a characteristic energy which depends on the percolation threshold of the lattice [15, 16], and frequency-dependent diffusion becomes universal if properly scaled [17]. The scaled units include information about different parameters: temperature, characteristic percolation energy, and a characteristic frequency that marks the onset of static diffusion.

In this paper we shall focus on the description of a model for anisotropic diffusion processes, both in the static and frequency-dependent regimes. In order to emphasize the role of temperature and its relevance for diffusion in a system with energy disorder, we use here a two-dimensional isotropic bond percolation system with different energy-dependent intrinsic transition rates in each direction. We define the transition rates as $w_{1(2)}$ in the 1(2) direction and choose them according to $\Gamma(w_1)$ and $\Omega(w_2)$, the probability distribution functions (PDFs), which for this anisotropic model are given by

$$\begin{aligned} \Gamma(w_1) &= p\delta(w_1 - w_1^0) + (1-p)\delta(w_1), \\ \Omega(w_2) &= p\delta(w_2 - w_2^0) + (1-p)\delta(w_2). \end{aligned} \tag{1}$$

It means that the transition rate w_1 takes the value w_1^0 with occupation probability p, and zero otherwise, and analogously for the 2 direction.

In order to account for the temperature dependence of diffusion coefficients, we propose intrinsic transition rates characterized by a thermally activated process with different activation energies in each direction. Therefore we define an *anisotropic thermally activated process*, in which the transition rates in each direction take the form

$$w_{1(2)}^0 = \gamma_0 \exp\left(-\frac{\epsilon_{1(2)}}{kT}\right), \tag{2}$$

where γ_0 is the constant jump rate and k is the Boltzmann constant. The $(1-p)$ fraction of non-conductor components in Eq. (1) now represents the existence of infinite energy barriers.

We set $\epsilon_1 > \epsilon_2$ and define an anisotropic parameter $\alpha = \epsilon_1/\epsilon_2$, and a mean energy $\epsilon = (\epsilon_1 + \epsilon_2)/2$. This mean energy was kept constant in the present work. In terms of these parameters we may write $\epsilon_1 = 2\alpha\epsilon/(\alpha+1)$ and $\epsilon_2 = 2\epsilon/(\alpha+1)$. Then, the relevant parameters of the problem become the occupation probability p, the temperature T, and the anisotropic parameter α. In the following, energies and temperatures are measured in arbitrary units (with $k = 1$).

The proposed model is studied both analytically, by using an anisotropic extension to the effective medium approximation (EMA), and numerically by means of standard Monte Carlo (MC) simulations. We shall briefly describe both methods.

The reader is referred to [5] for a complete description of anisotropic EMA. Here we only summarize the key results. The EMA consists in averaging the effects

of disorder by defining an effective medium with effective transition rates, which depend on the Laplace variable u. These effective transition rates are self-consistently determined by the requirement that the difference between the propagator of the impurity and homogeneous problems should average to zero. Thus, in anisotropic problems, two effective transition rates, $w_1^e(u)$ and $w_2^e(u)$ (one for each direction), are introduced. These effective transition rates are determined by two self-consistent conditions [4, 5]:

$$\left\langle \frac{w_1^e - w_1}{1 + 2\,(w_1^e - w_1)\,[G^1(u) - G^0(u)]} \right\rangle_{\Gamma(w_1)} = 0,$$
$$\left\langle \frac{w_2^e - w_2}{1 + 2\,(w_2^e - w_2)\,[G^2(u) - G^0(u)]} \right\rangle_{\Omega(w_2)} = 0. \quad (3)$$

Here, $G^{1(2)}$ and G^0 are the non-perturbed anisotropic Green functions related to the probabilities of moving from the origin to one of its nearest neighbors in the 1(2) direction and the return probability, respectively. The impure bond connects two nearest neighbor sites of the lattice whose transition rates are equal to w_1 if the impure bond lies in the 1 direction and w_2 if the impure bond is in the other direction.

Following the linear response theory [18] the generalized frequency-dependent complex diffusion coefficients $D(\omega)$ in the anisotropic EMA context are given by $D_{1(2)}(\omega) = a^2\, w^e_{1(2)}(u = i\omega)$, where a is the lattice constant. In the following we will take $a = 1$.

In the static case ($\omega = 0$) Eqs. (3) become

$$\frac{2}{\pi}\left[D_1^0 - \gamma_0 \exp\left(-\frac{\epsilon_1}{kT}\right)\right] \arctan\sqrt{\frac{D_1^0}{D_2^0}} + p\gamma_0 \exp\left(-\frac{\epsilon_1}{kT}\right) = 0,$$
$$\frac{2}{\pi}\left[D_2^0 - \gamma_0 \exp\left(-\frac{\epsilon_2}{kT}\right)\right] \arctan\sqrt{\frac{D_2^0}{D_1^0}} + p\gamma_0 \exp\left(-\frac{\epsilon_2}{kT}\right) = 0, \quad (4)$$

where the transition rates are defined in Eq. (2), $D_1^0 = D_1(\omega = 0) = w_1^e(0)$ and $D_2^0 = D_2(\omega = 0) = w_2^e(0)$ represent zero-frequency (static) diffusion coefficients in each direction.

Monte Carlo data are obtained by performing classical random walk simulation in square lattices with 300^2 sites. Normal diffusion regime (long-time limit) is reached between 10^3 and 10^6 steps, and the mean square displacement is averaged over 2000 and 10000 different lattices, depending on data fluctuations. Static diffusion coefficients are obtained via the Einstein's relations, $\left\langle R^2_{1(2)} \right\rangle = 2D^0_{1(2)}t$. As was shown earlier [19], standard MC simulations fail to describe particle diffusion for very low temperatures. In this limit the method is inefficient and other simulation methods are necessary. Here the standard MC method was used and simulations were performed for temperatures above $T = 0.05$.

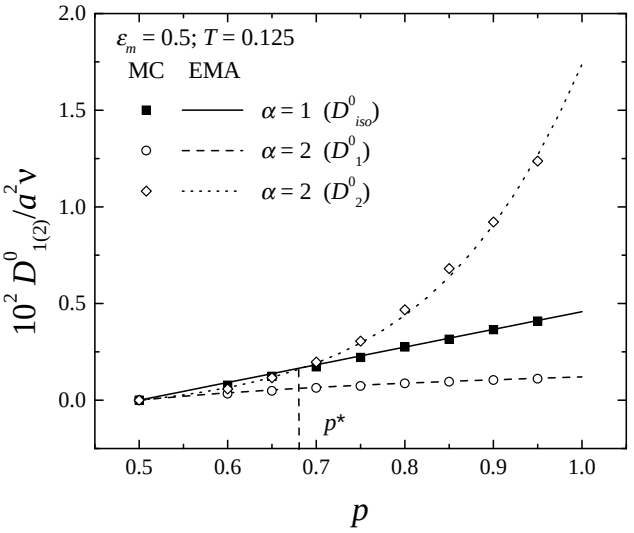

FIG. 1: Dependence of the anisotropic static diffusion coefficients on the occupation probability p for $T = 0.125$. The characteristic value p^* is also indicated. Energy and temperature are given in arbitrary units with the Boltzmann constant $k = 1$.

We present now the results for the long-time diffusion properties. Firstly, in the isotropic case $\alpha = 1$, the transition rates are given by $\gamma_0 \exp\left(-\frac{\epsilon}{kT}\right)$ and, as expected, only one diffusion coefficient is obtained, viz., $D^0_{iso} = D^0_1 = D^0_2 = \gamma_0 \exp\left(-\frac{\epsilon}{kT}\right)(2p - 1)$. Secondly, for all values of α, in the $T \to \infty$ limit ($kT \gg \epsilon$) the model again reduces to the isotropic bond percolation problem with transition rates γ_0 [Eq. (2)]. In this case, the isotropic diffusion coefficient is given by $D^0_{iso} = \gamma_0(2p - 1)$. Finally, for values of $\alpha \neq 1$ and in the low temperature limit D^0_1 and D^0_2 were calculated by numerically solving the set of Eqs. (4), and results are compared with MC simulations.

Let us consider the variation of D^0_1 and D^0_2 with the occupation probability p, for fixed values of T in anisotropic conditions. The calculation was performed for $\epsilon = 0.5$ and $\gamma_0 = 0.25\nu$, where ν is a characteristic jump frequency. Figure 1 shows $D^0_{1(2)}$ as a function of p for $T = 0.125$. Symbols represent MC simulations and lines correspond to the EMA numerical solution of Eqs. (4). The isotropic $\alpha = 1$ case is included for comparison. For $\alpha > 1$, we obtain $D^0_1 < D^0_2$, which is in agreement with the fact that lower energy barriers imply higher diffusion coefficients. For $p \leq p_c = 0.5$, the isotropic bond percolation threshold [13], we find that $D^0_1 = D^0_2 = 0$ as expected. In the low p region the two anisotropic diffusion coefficients are lower than the isotropic one ($p \leq p^* \simeq 0.68$). In this region the conducting cluster is poorly connected and the diffusion in the low energy direction is highly affected by the existence and height of high energy barriers. As p is increased, more energy barriers appear and the diffusion in the low energy barrier direction is less sensitive to high energy barriers. This

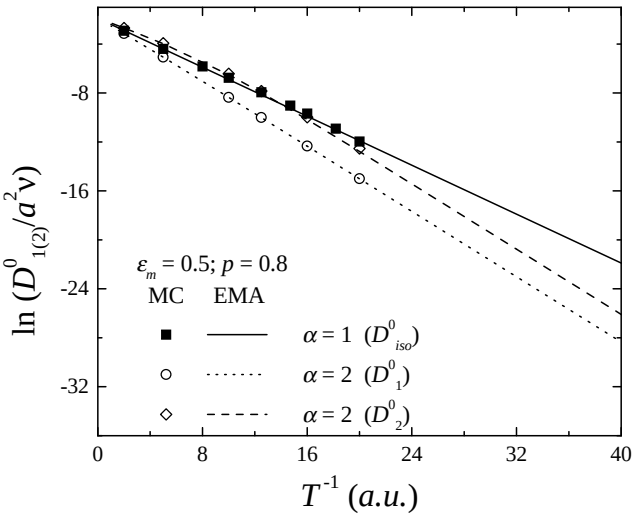

FIG. 2: Arrhenius plot for the anisotropic static diffusion coefficients at low temperatures for $p = 0.8$. Energy and temperature are given in arbitrary units with the Boltzmann constant $k = 1$.

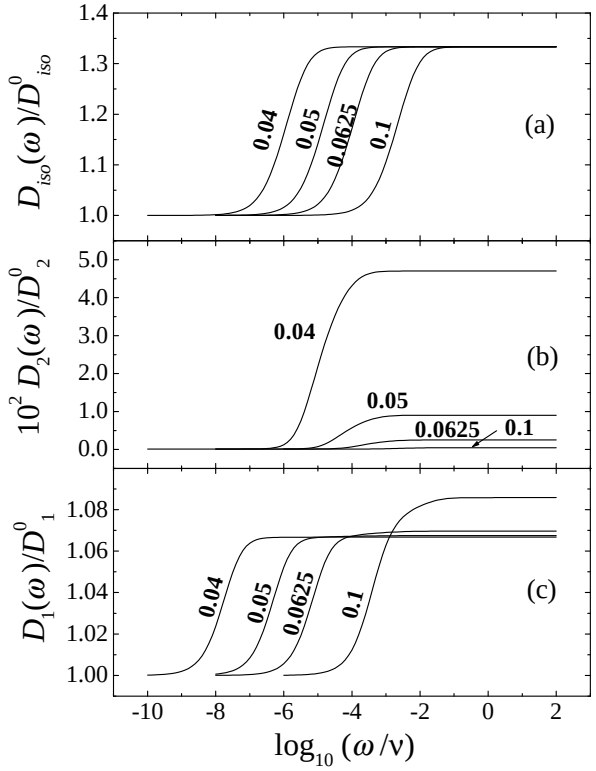

FIG. 3: Scaled frequency-dependent diffusion coefficients for isotropic (a) and anisotropic $\alpha = 2$ [(b) and (c)] cases. Each curve is labeled with its corresponding temperature (in arbitrary units).

kind of behavior is also found for other values of T, with increasing values of p^* as T decreases.

Next we turn to the behavior of D^0_1 and D^0_2 at low temperatures for fixed values of p. We do not present here results for $p = p_c$ (or near p_c), the percolation threshold, where the substrate has fractal properties and diffusion becomes anomalous [1, 2]. In Fig. 2 we show the temperature dependence of the static diffusion coefficients in an Arrhenius plot for $p = 0.8$ and $\alpha = 1$ and 2. From the EMA curves (lines) the slope of the linear region is numerically calculated. For isotropic media, the EMA predicts a slope equal to $-0.5 = -\epsilon$. For $\alpha = 2$, we find that $D^0_1(T)$ and $D^0_2(T)$ reach an asymptotic Arrhenius behavior with the same activation energy ϵ_1, corresponding to the highest energy of this anisotropic model. This is not a striking result considering that long-time diffusion at low temperatures is strongly governed by the highest energy barrier, as the particle spends a lot of time trying to overcome them while performing long-distance trajectories. The low temperature behavior of static diffusion coefficients depends only on the highest characteristic energy value of this anisotropic model.

The frequency behavior of diffusion coefficients was studied by numerically solving the set of coupled Eqs. (3), using the corresponding expressions for the anisotropic Green functions [5], and the temperature dependence introduced in Eq. (2). We present here results for the real part of the frequency-dependent complex diffusion coefficients. In Fig. 3 we show the scaled values $D_{1(2)}(\omega)/D^0_{1(2)}$ for $p = 0.8$, $\epsilon = 0.5$, and temperature values between 0.1 and 0.04. Three characteristic regimes can be distinguished: (i) the long-time limit for $\omega \to 0$, (ii) a power law behavior characteristic of intermediate frequencies, $\sigma \sim \omega^s$, with $s \leq 1$ and, (iii) the high-frequency regime, $\omega \to \infty$, where the diffusion coefficients approach to a constant value. This kind of dielectric response has been observed before in a broad class of ionic and electronic systems, in isotropic and anisotropic media [17, 20, 21].

In the isotropic case we find that while decreasing the temperature the scaled value $D_{iso}(\omega)/D^0_{iso}$ reaches a temperature-independent value for $\omega \to \infty$ [Fig. 3 (a)]. In the anisotropic case, while $D_1(\omega)/D^0_1$ saturates for $\omega \to \infty$ to a temperature-independent value at low temperatures [Fig.3 (c)], $D_2(\omega)/D^0_2$ saturates to a temperature-dependent value that follows an Arrhenius law with an activation energy equal to $\epsilon_1 - \epsilon_2$, even at low temperatures [Fig.3 (b)]. This $\omega \to \infty$ behavior can be interpreted from the evolution of the particle diffusion for $t \to 0$. For $\alpha = 1$ we find that $D_{iso}(\omega \to \infty) = p\gamma_0 \exp\left(-\frac{\epsilon}{kT}\right)$. This means that the first step of the particle is given by the probability p of finding a given bond times the intrinsic transition rate of that bond. From this considerations and using the isotropic result for $D^0_{iso}(T)$ we find that $D_{iso}(\omega \to \infty)/D^0_{iso} = p/(2p-1) = 4/3$ for $p = 0.8$, as shown in Fig. 3 (a). In anisotropic conditions, we expect the $t \to 0$ ($\omega \to \infty$) evolution to be given by $p\gamma_0 \exp\left(-\frac{\epsilon_1}{kT}\right)$ in the 1 direction and by $p\gamma_0 \exp\left(-\frac{\epsilon_2}{kT}\right)$ in the 2 direction. We showed pre-

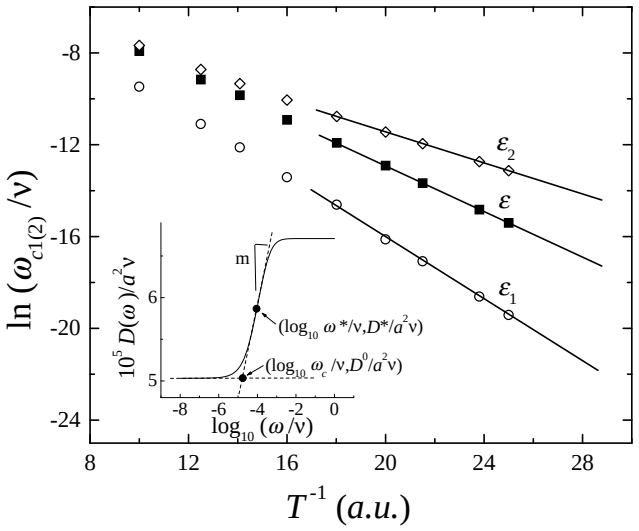

FIG. 4: Temperature dependence of the characteristic frequencies $\omega_{c1(2)}$. The isotropic case $\omega_{c,iso}$ (full squared) and the anisotropic $\alpha = 2$ cases ω_{c1} (open circles) and ω_{c2} (open diamond) are shown. Lines are guides to the eye and are labeled by its corresponding activation energy. The inset shows the determination of the value ω_c from a typical curve for the frequency-dependent diffusion coefficient. The value m represent the slope of the tangent curve through the inflection point $(\log_{10}\omega^*/\nu, D^*/a^2\nu)$ (see text).

viously that $D_1^0 \sim \exp\left(-\frac{\epsilon_1}{kT}\right)$, and $D_2^0 \sim \exp\left(-\frac{\epsilon_1}{kT}\right)$, thus $D_1(\omega\to\infty)/D_1^0$ is expected to be constant at low temperatures, and $D_2(\omega\to\infty)/D_2^0 \sim \exp\left(\frac{\epsilon_1-\epsilon_2}{kT}\right)$, which account for the calculated EMA results for $\omega\to\infty$ in Fig. 3 (b) and (c).

For intermediate frequencies a characteristic frequency $\omega_c \sim 1/t_c$ can be defined, related to the time t_c needed to overcome a characteristic energy barrier. The inset of Fig. 4 shows a typical frequency-dependent $D(\omega)$ plot (as those in Fig. 3). The ω_c parameter is calculated from our anisotropic EMA data as follows. Let the inflection point be $(\log_{10}\omega^*/\nu, D^*/a^2\nu)$, and m the slope of the tangent curve passing through the inflection point. The $\omega_{c1(2)}$ parameter is given by the intersection of the slope m through the inflection point and the line corresponding to the long-time diffusion coefficient $D^0_{1(2)}$ (Fig. 4, inset). We include the subscript 1(2) as ω_c may be different for each direction. In Fig. 4 we present the temperature dependence of the characteristic frequencies $\omega_{c1(2)}$ in an Arrhenius plot for $\alpha = 1$ and 2. All cases reach a linear behavior for low temperature values, but different slopes are found in each case, corresponding to the characteristic energy in each direction. This indicates, as expected, that different times $t_{c1(2)} \sim \exp\left(-\frac{\epsilon_{1(2)}}{kT}\right)$ are needed in each direction to overcome its characteristic energy barriers.

In summary, in the present paper we described long-time and frequency-dependent diffusion in anisotropic thermally activated processes in a two-dimensional bond percolation lattice. The present model has different activation energies in each direction of the square lattice. Long-time diffusion coefficients follow an Arrhenius law at low temperatures with the highest energy barrier being the activation energy for diffusion in both directions of the lattice. From the frequency-dependent diffusion coefficients, we define a characteristic frequency $\omega_{c1(2)}$. We remark that ω_c is not marking the onset of long-time diffusion, as in isotropic problems with continuous PDFs [17], but it is just the frequency associated to overcome the characteristic energy of *each* direction. The existence of two different activation energies for $\omega_{c1(2)}$ and only one for $D^0_{1(2)}$ is a consequence of the strength of the percolation-type disorder, in contrast with results from isotropic continuous PDFs, where the characteristic frequency and the static diffusion coefficient follow Arrhenius laws *with the same* activation energy [15, 16, 17].

S. B. thanks a fellowship from Universidad Nacional del Comahue at the early stages of this work. This work was partially suported by Universidad Nacional del Comahue and CONICET.

[1] J. W. Haus and K. W. Kehr, Phys. Rep. **150**, 263 (1987).
[2] J. P. Bouchaud and A. Georges, Phys. Rep. **195**, 127 (1990).
[3] M. Sahimi, *Flow and Transport in Porous Media and Fractured Rock* (VCH, Weinheim, Germany, 1995).
[4] P. E. Parris, Phys. Rev. B **36**, 5437 (1987).
[5] E. R. Reyes, M. O. Cáceres, and P. A. Pury, Phys. Rev. B **61**, 308 (2000).
[6] M. O. Cáceres and E. R. Reyes, Physica A **227**, 277 (1996).
[7] S. Bustingorry, E. R. Reyes, and M. O. Cáceres, Phys. Rev. E **62**, 7664 (2000).
[8] M. Saadatfar and M. Sahimi, Phys. Rev. E **65**, 036116 (2002).
[9] S.-Y. Huang, X.-W. Zou, and Z.-Z. Jin, Phys. Rev. E **65**, 052105 (2002).
[10] J. M. V. A. Koelman and A. de Kuijper, Physica A **247**, 10 (1997).
[11] A. Celzard *et al.*, Solid State Commun. **92**, 377 (1994).
[12] L. K. Gallos, A. N. Anagnostopoulos, and P. Argyrakis, Phys. Rev. B **50**, 14643 (1994).
[13] D. Stauffer and A. Aharony, *Introduction to Percolation Theory* (Taylor & Francis, London, 1994).
[14] G. Grimmet, *Percolation* (Springer-Verlag, Berlin, 1990).
[15] A. Hörner, A. Milchev, and P. Argyrakis, Phys. Rev. E **52**, 3570 (1995).
[16] P. Argyrakis, A. Milchev, V. Pereyra, and K. W. Kehr, Phys. Rev. E **52**, 3623 (1995).
[17] J. C. Dyre and T. B. Schroder, Rev. Mod. Phys. **72**, 873 (2000).
[18] T. Odagaki and M. Lax, Phys. Rev. B **24**, 5284 (1981).
[19] J. C. Dyre, Phys. Rev. B **49**, 11709 (1994).

[20] H. Jhans, D. Kim, R. J. Rasmussen, and J. M. Honig, Phys. Rev. B **54**, 11224 (1996).

[21] C. A. Angell, Chem. Rev. **90**, 523 (1990).